ELSEVIER

Journal of Photochemistry and Photobiology A: Chemistry 107 (1997) 47–54

Journal of PHOTOCHEMISTRY AND PHOTOBIOLOGY A:CHEMISTRY

Bimolecular photoinduced electron transfer in the Marcus inverted region involving the $[Re(CO)_3(4\text{-phenylpyridine})_3]^+$ metal-to-ligand charge transfer excited state, amines and their corresponding radical products

G. Ruiz [1], F. Rodriguez-Nieto, E. Wolcan [2], M.R. Féliz *

Instituto de Investigaciones Fisicoquimicas Teóricas y Aplicadas (INIFTA), Facultad de Ciencias Exactas-Universidad Nacional de La Plata,
C.C. 16, SUC. 4, (1900) La Plata, Argentina

Received 6 November 1996; accepted 28 January 1997

Abstract

Bimolecular electron transfer quenching of the metal-to-ligand charge transfer (MLCT) excited state of $Re(CO)_3$(4-phenylpyridine)$_3$(F_3CSO_3) by amines was studied in acetonitrile at room temperature. The quenching rate constants (k_q) vary from 1.8×10^7 to 2.5×10^{10} M^{-1} s^{-1} (diffusion limit). Moreover, the radical recombination reaction (back electron transfer) was also studied by flash photolysis. The back electron transfer rate constants range from 2.8×10^5 to 7.0×10^9 M^{-1} s^{-1}, lying below the diffusion-controlled limit. The rate constants show an inverse dependence on the driving force in the inverted region. All the data points can be fitted using a semiclassical model. © 1997 Elsevier Science S.A.

Keywords: Amines; Bimolecular electron transfer; Quenching; Rate constants; Rhenium

---

1. Introduction

More than three decades ago, Marcus predicted that there should be an inverted region for electron transfer [1]. Electron transfer theory, formulated classically or by time-dependent perturbation theory, results in the electron transfer rate constant being the product of three factors: electronic factors, changes in vibrational displacement and a temperature-dependent solvent distribution. In the classical limit, for reactions in condensed media, theory predicts a bell-shaped Gibbs energy–rate relationship: rate constants are expected to be small for weakly exothermic reactions, increase to a maximum for moderately exothermic reactions (the "normal region") and decrease for highly exothermic electron transfer reactions in the so-called "inverted region". Confirmation of the "inverted effect" took about 25 years [2]. Since then the "inverted region" has been observed experimentally in many electron transfer systems [3–8]. However, very few examples of bimolecular electron transfer reactions showing more than "vestiges" of the "inverted effect" have been found [9]. In this paper, we report a bimolecular electron transfer reaction in solution which displays inverted behaviour.

2. Experimental section

2.1. Materials

fac-$[Re(CO)_3(4\text{-phenylpyridine})_3](F_3CSO_3)$ was prepared according to a literature procedure [10]. The amine quenchers purchased from Aldrich were of the highest purity available. When required they were purified by distillation. The pure amines were handled under nitrogen. Tetrabutylammonium hexafluorophosphate from Aldrich was recrystallized from ethanol and vacuum dried before use. Acetonitrile (OmniSolv) from EM Science and tetrabutylammonium iodide from Aldrich were used as received.

2.2. Quenching measurements

Samples for quenching measurements in acetonitrile contained $Re(CO)_3(4\text{-phpy})_3^+$ (5×10^{-5} M) (4-phpy, 4-phenylpyridine) with the appropriate concentration of added

---

* Corresponding author. Fax: +54 21 254642.

[1] G. Ruiz, F. Rodriguez-Nieto and M.R. Féliz are members of the Comisión de Investigaciones Científicas de la Provincia de Buenos Aires (CICBA).

[2] Member of the Consejo Nacional de Investigaciones Científicas y Técnicas de la República Argentina (CONICET).

1010-6030/97/$17.00
PII S1010-6030(97)00059-2

quencher. In a typical experiment, solutions containing five to ten different concentrations of quencher were placed in a gas-tight quartz cell. The solutions were deaerated by bubbling with oxygen-free nitrogen for 15–30 min. Emission measurements were made using an SLM 4800 spectrofluorometer or the total fluorescence accessory of a Cary 3 spectrophotometer. No differences were observed in the results obtained using this equipment.

2.3. Flash photolysis

Flash photolysis experiments were carried out on solutions which had been deaerated with O_2-free purified nitrogen. The solutions contained $Re(CO)_3(4\text{-phpy})_3^+$ (5.0×10^{-5} M) and amine (1.0×10^{-3} M). The wavelength region above 320 nm was isolated by means of a cut-off filter (acetone). The modified Xenon Co. flash spectrophotometer used has been described elsewhere [11].

2.4. Electrochemical measurements

Cyclic voltammetric measurements on the amine quenchers and rhenium complex were performed in acetonitrile solutions at a glassy carbon working electrode with 0.1 M tetrabutylammonium hexafluorophosphate as supporting electrolyte. The compound concentration was kept at 1.0×10^{-3} M in all the experiments. The ferrocene/ferricinium couple was used as the standard for all the experiments.

Table 1 lists the E_{peak} values of the oxidation potentials vs. SSCE for the amines. It is important to note that most of the compounds present no reversible redox couple (see Section 3). However, our results are in good agreement with those reported in the literature [12–15]. The rhenium complex is a reversible one-electron couple with $E_{1/2}=-1.61$ V.

3. Results and discussion

3.1. Forward electron transfer

The reductive quenching of the rhenium complex metal-to-ligand charge transfer (MLCT) excited state by amines produces the oxidized form of the amine and the reduced radical of the rhenium complex [16–18]

$$[Re(CO)_3(4-phpy)_3^+]^* + \text{amine} \xrightarrow{k_q} Re(CO)_3(4-phpy)_3^{\cdot} + \text{amine}^+ \qquad (1)$$

The results of the quenching experiments are shown in Table 1. The data were plotted according to the Stern–Volmer equation

$$I_0/I = 1 + k_q\tau_0[\text{amine}] \qquad (2)$$

where k_q is the experimental quenching rate constant, τ_0 is the excited state lifetime of $[Re(CO)_3(4\text{-phpy})_3^+]^*$ and I_0 and I are the luminescence intensities in the absence and presence of quencher respectively. The plots were linear over the range of quencher concentrations used and the intercepts were unity as expected (Fig. 1). The k_q values were determined from the slopes of the lines using $\tau_0=2.2$ μs for $[Re(CO)_3(4\text{-phpy})_3^+]^*$ in acetonitrile [16].

3.2. Back electron transfer

The rate constant k_{back} for the back electron transfer reaction

$$Re(CO)_3(4-phpy)_3^{\cdot} + \text{amine}^+ \rightarrow Re(CO)_3(4-phpy)_3^+ + \text{amine} \qquad (3)$$

was determined by flash photolysis experiments. It is known [16,17] that the rhenium radical produced by quenching of

Table 1
Rate constants for the excited state quenching reaction of $Re(CO)_3(4\text{-phpy})_3^+$ with amines

Quencher	E_{ox} (V) [a]	r_D (Å) [b]	k_q ($M^{-1}s^{-1}$)	k_{back} ($M^{-1}s^{-1}$)
Tetrakis(dimethylamino)ethylene	−0.63	5.0	1.1×10^{10}	
1,4-Phenylenediamine	0.34	4.5	2.6×10^{10}	
p-Benzidine	0.56	6.6	1.6×10^{10}	
DABCO	0.56	3.6	1.4×10^{10}	7.0×10^{9}
N,N,N',N'-Tetramethylethylenediamine	0.87	4.9	3.7×10^{9}	1.0×10^{6}
N,N-Diisopropylethylamine	0.88	4.6	9.2×10^{9}	
Tripentylamine	0.89	8.4	6.6×10^{9}	8.0×10^{6}
Triethanolamine	0.90	4.8	1.9×10^{9}	1.3×10^{7}
Triethylamine	0.99	4.3	2.7×10^{9}	4.6×10^{6}
N,N-Dimethylethylamine	1.05	3.9	1.9×10^{9}	
N,N,N',N'-Tetramethyldiaminomethane	1.06	4.5	7.5×10^{8}	1.4×10^{7}
Aniline	1.08	4.1	2.8×10^{9}	1.4×10^{7}
Piperidine	1.30	3.7	8.2×10^{8}	2.8×10^{5}
4-Dimethylaminopyridine	1.45	4.4	1.8×10^{7}	

[a] Oxidation potential of quencher vs. SSCE in CH_3CN.
[b] Quencher radius in angstrom.

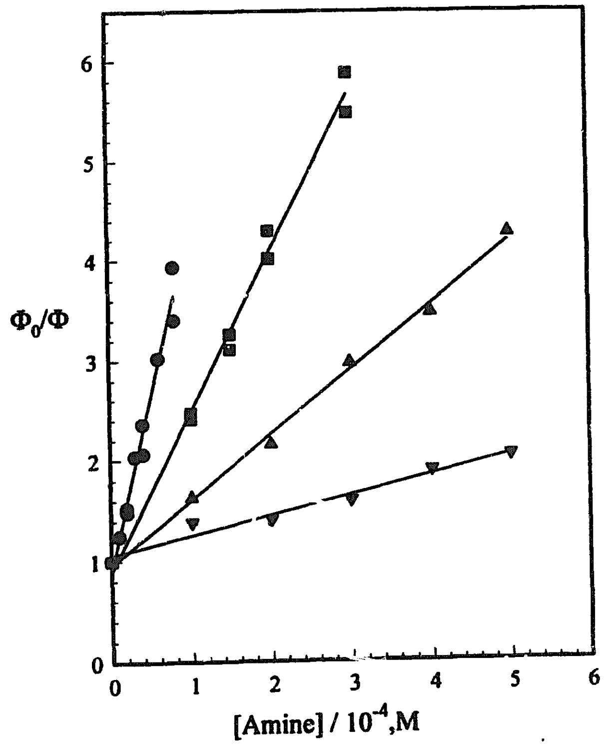

Fig. 1. Stern–Volmer kinetics of the luminescence quenching of $[Re(CO)_3(4\text{-phenylpyridine})_3^+]^*$ with amines: DABCO (●), tripentylamine (■), triethylamine (▲) and piperidine (▼).

the MLCT excited state with amines in acetonitrile solution disappears by reactions (3) and (4)

$$Re(CO)_3(4-phpy)_3^{\cdot} \rightarrow \text{products} \qquad (4)$$

The curve-fitting analysis of the radical decay at 560 nm is consistent with competition between first-order and second-order kinetics. All the rate constants reported in this paper for the back electron transfer reaction were calculated using software designed in our laboratory for non-linear multiparametric kinetic analysis [19] assuming the mechanism of Eqs. (3) and (4). In these experiments, the initial concentration of the amine was 1×10^{-3} M. The second-order rate constants were not affected by the flash intensity (i.e. the initial concentration of the radicals) within experimental error while varying the capacitor voltage between 4 and 9 kV and the capacitances between 5 and 20 μF. Experiments carried out at different initial concentrations of the amine quencher (between 7×10^{-4} and 1×10^{-2} M) showed that the second-order rate constants remained almost unaffected.

To obtain the actual second-order rate constant k_{back}, the rhenium radical extinction coefficient must be determined. For this purpose, acetonitrile solutions containing $Re(CO)_3(4\text{-phpy})_3^+$ (1×10^{-4} M) and tetrabutylammonium iodide (1×10^{-3} M) were flash photolysed using acetone as a cut-off filter. Taking into account literature reports [20], the events occurring after the flash can be summarized as follows

$$Re(CO)_3(4-phpy)_3^+ + h\nu \rightarrow [Re(CO)_3(4-phpy)_3^+]^* \qquad (5)$$

$$[Re(CO)_3(4-phpy)_3^+]^* + I^- \rightarrow Re(CO)_3(4-phpy)_3^{\cdot} + I \qquad (6)$$

$$I + I^- \rightleftarrows I_2^- \qquad (7)$$

$$I + I \rightarrow I_2 \qquad (8)$$

$$I + I_2^- \rightarrow I_3^- \qquad (9)$$

$$I_2^- + I_2^- \rightarrow I_3^- + I^- \qquad (10)$$

$$Re(CO)_3(4-phpy)_3^{\cdot} \rightarrow \text{products} \qquad (11)$$

Rhenium radical and I_2^- spectra (Fig. 2) present absorption maxima at different wavelengths. At 560 nm, the radical decays by first-order kinetics and I_2^- shows a second-order decay at 750 nm. The spectra were extrapolated to $t = 0$ using a fitting program developed in our laboratory. It is reasonable to assume [20] that the magnitudes of the individual bimolecular rate constants for reactions (7)–(10) are comparable, and since under our conditions the iodide ion concentration (1×10^{-3} M) is several powers of ten larger than the concentration of I and I_2^- (approximately 1×10^{-7} M), it is a good approximation to assume that the rates of the reactions which establish equilibrium are much larger than the rates of the reactions by which I and I_2^- disappear. Indeed, the equi-

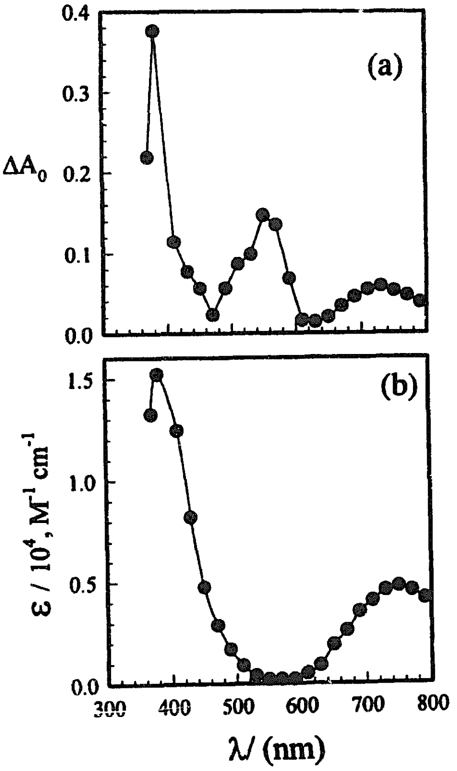

Fig. 2. Determination of the rhenium radical extinction coefficient: (a) difference spectrum obtained in flash photolysis experiments using acetonitrile solutions of $Re(CO)_3(4\text{-phenylpyridine})_3^+$ (1×10^{-4} M) and tetrabutylammonium iodide (1×10^{-3} M) with acetone as cut-off filter; (b) spectrum of I_2^- species [20].

librium constant for I_2^- formation is very large, with a value of 1.1×10^5 M^{-1} [21]. As a result, the initial concentration of I_2^- will not differ substantially from the initial concentration of I (which is equal to the initial concentration of $Re(CO)_3(4\text{-phpy})_3^{\cdot}$ from Eq. (6)), since the equilibrium will be strongly displaced to the right in Eq. (7). As the initial concentrations of both intermediates are nearly equal and the extinction coefficient for I_2^- is $\epsilon_I(750\,\text{nm}) = 4741$ M^{-1} cm^{-1} [20], the corresponding rhenium radical extinction coefficient can be obtained, $\epsilon_r(560\,\text{nm}) = 13\,800$ M^{-1} cm^{-1}. The values of k_{back} are listed in Table 1. It is important to note that I_2^- does not react with the Re radical as shown by the first-order decay. This provides further evidence that the second-order process observed in the presence of the amine corresponds to reaction (3).

3.3. Spectral analysis

In order to obtain the zero–zero energy difference (E_{00}), the corrected emission spectra [22] of the rhenium complex were fitted according to Eqs. (12) and (13) [23]

$$I(\nu) = \sum_{\upsilon_M}^{\infty}\sum_{\upsilon_L}^{\infty}[(\nu_{00} - \upsilon_M\nu_M - \upsilon_L\nu_L)/\nu_{00}]^4 \times [(S_M^{\upsilon_M})/\upsilon_M!] \times [(S_L^{\upsilon_L})/\upsilon_L!] \times \exp\{-4(\ln 2)[(\nu - \nu_{00} + \upsilon_M\nu_M + \upsilon_L\nu_L)/\Delta\nu_{1/2}]^2\} \qquad (12)$$

$$I_{\text{em}}(\nu)/I_{\text{em}}(\nu_{\text{max}}) = N \times I(\nu) \qquad (13)$$

where $I_{\text{em}}(\nu)$ and $I_{\text{em}}(\nu_{\text{max}})$ represent the observed emission intensities at frequency ν (in cm^{-1}) and ν_{max} (the frequency of the emission maximum) respectively. In Eq. (12), υ_M and υ_L are the vibrational quantum numbers for high-frequency (ν_M) and low-frequency (ν_L) vibrational progressions of the acceptor modes. In the band shape equation, $I(\nu)$ is the intensity of the $\upsilon_M^* = 0$, $\upsilon_L^* = 0$ to $\upsilon_M = n_M$, $\upsilon_L = n_L$ transition relative to the intensity of the $\upsilon_M^* = 0$, $\upsilon_L^* = 0$ to $\upsilon_M = 0$, $\upsilon_L = 0$ transition, the so-called 0–0 transition, ν_{00}. The summation was carried out over six levels of vibrations ν_M and ν_L ($\upsilon_M = 0 \rightarrow 5$ and $\upsilon_L = 0 \rightarrow 5$). S_M and S_L are the electron vibrational coupling constants for the high- and low-frequency modes respectively and $\Delta\nu_{1/2}$ is the full width at half-maximum of the 0–0 vibrational component of the emission. N is a constant introduced in the fitting equation due to the shift between ν_{max} and ν_{00}. Thus the fitting process involves the determination of seven parameters, namely ν_{00}, ν_M, ν_L, S_M, S_L, $\Delta\nu_{1/2}$ and N. For the purpose of spectral fitting, the emission spectra were converted from having an abscissa linear in wavelength, which is characteristic of the emission spectrometer used, to an abscissa linear in energy by the method described in the literature [23]. The results of the fitting process for room temperature (RT) and 77 K emissions are shown in Fig. 3 and Table 2.

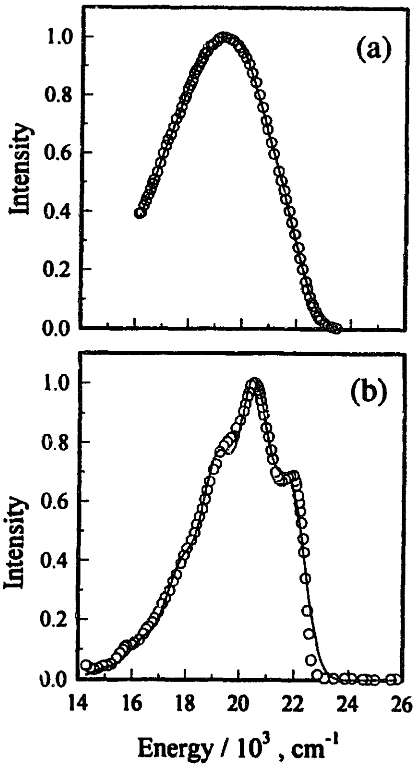

Fig. 3. Spectral analysis of the room temperature (a) and 77 K (b) corrected emission spectra of the rhenium complex. The open circles represent the experimental emission data and the full lines the calculated fits according to Eqs. (12) and (13) using the spectral parameters in Table 2.

3.4. Estimation of the free energy (ΔG)

The energy balance of the forward electron transfer is given by

$$\Delta G = E_{\text{ox}} - E_{\text{red}} - E_{00} - e^2/\epsilon r \qquad (14)$$

where E_{ox} is the donor (amine) oxidation potential, E_{red} is the acceptor reduction potential, E_{00} is the energy of the excited state, e is the charge of an electron, ϵ is the static dielectric constant of the solvent and r is the distance between the two reactants. The last term ($-e^2/\epsilon r$) represents the static attraction energy of the products. In the same way, the energy balance for back electron transfer is given by

$$\Delta G_{\text{back}} = E_{\text{red}} - E_{\text{ox}} + e^2/\epsilon r \qquad (15)$$

In both cases, the Coulomb term can be neglected because one of the reactants has no charge.

3.5. Relationship between the rate constants and ΔG

In Fig. 4, $RT \ln k_j$ (j = q, back) is plotted against ΔG. For the forward reaction, the rate constants increase as the driving force becomes less positive (normal region). However, when $-\Delta G = 0.9$ eV, k_q reaches the diffusional value k_d and, at more negative values ($-\Delta G = 1.95$ eV), it shows "vestiges" of inverted region behaviour. The k_q value is not appreciably lower than k_d, a situation often encountered in studies

Table 2
Emission spectral fitting parameters for $Re(CO)_3(4\text{-phpy})_3^+$ [a]

Temperature	E_{00} (cm^{-1})	ν_M (cm^{-1})	ν_L (cm^{-1})	S_M	S_L	$\Delta\nu_{1/2}$ (cm^{-1})	N
77 K	21890 ± 22	1357 ± 30	500 ± 300	1.92 ± 0.08	0.22 ± .15	1250 ± 70	0.56 ± 0.03
Room temperature	21330 ± 56	1420 ± 24	500 ± 173	2.42 ± 0.07	0.20 ± 0.008	1810 ± 70	0.36 ± 0.01

[a] Based on a seven parameter fit using Eqs. (12) and (13).

of bimolecular electron transfer reactions at high exothermicities. The system goes into the inverted region when $\Delta G = -\lambda$, i.e. for the present case at approximately -1.1 eV (see below). As in the electron transfer quenching reaction, the chemical redox energy stored is considerable and back electron transfer is highly favourable ($-\Delta G° > \lambda$) and falls deeply in the Marcus inverted region. In this case, k_{back} decreases as $-\Delta G$ increases as predicted theoretically.

3.6. Classical treatment

The usual mechanism can be considered for the forward and backward reactions

$$A^{+*} + D \underset{k_{-d}}{\overset{k_d}{\rightleftharpoons}} A^{+*}----D \underset{k_{-e}}{\overset{k_e}{\rightleftharpoons}} A----D^{+} \xrightarrow{k_p} A + D^{+}$$

where k_d is the diffusion rate constant, k_{-d} is the dissociation rate constant, k_e and k_{-e} are the forward and backward electron transfer rate constants and k_p is the rate constant for pair separation. Under the assumption that k_p is much larger than k_{-e}, the overall rate constant is written as [24]

$$k_j = k_d/(1 + k_{-d}/k_e) \qquad (16)$$

Rewriting k_j as a function of ΔG, we obtain [25]

$$k_j = k_d/\{1 + (k_d/\kappa\nu_N K_d)\exp[(\lambda + \Delta G)^2/4\lambda RT]\} \qquad (17)$$

where κ is the transmission coefficient of electron transfer, ν_N is the frequency factor, K_d is the equilibrium constant of the encounter complex ($K_d = k_d/k_{-d}$) and $\lambda/4$ is the activation free energy when $\Delta G = 0$ (intrinsic barrier). Here λ is considered to be the sum of the inner-sphere (λ_i) and solvent (λ_{out}) reorganization energy

$$\lambda = \lambda_i + \lambda_{out} \qquad (18)$$

According to literature reports [26], the factor ν_N varies from the order of 10^{12} to 10^{14} s^{-1}. We approximate it to be of the order of 10^{13} s^{-1}. The solvent reorganization energy λ_{out} is estimated by [27]

$$\lambda_{out} = e^2[1/2r_D + 1/2r_A - 1/r_{AD}][1/n^2 - 1/\epsilon] \qquad (19)$$

where r_D and r_A are the radii of the donor and acceptor, r_{AD} is the distance between the donor and acceptor in the encounter complex, n is the refractive index of the solvent (1.34 for acetonitrile at 298 K [28]) and ϵ is the solvent dielectric constant (37.5 for acetonitrile at 298 K [29]). Then, λ_{out} is estimated to be 0.674 eV. The radii of the amines have been estimated using a molecular modelling program which gives the geometry of minimal energy. For the complex, $r_A = 8.1$ Å was calculated using the interatomic distances obtained for fac-$Re(CO)_3(quinoline)_2Cl$ [30] and the radius of 4-phenylpyridine. The radii for the amines r_D are shown in Table 1. To calculate λ_{out}, a mean value of r_D was taken for the amines.

The diffusion rate constant (k_d), calculated according to Smoluchowski [31] for non-charged molecules, has a value of 2.0×10^{10} M^{-1} s^{-1} (since, for this system, the term $e^2/\epsilon r$ can be neglected, no distance effect on k_d was taken into account). However, the value 2.5×10^{10} M^{-1} s^{-1} has been used in this work, which is the maximum value for k_q. This value has already been used previously [9]. K_d was estimated following the Fuoss and Eigen equation [32], leading to the value of 5.44 M^{-1}. By fitting the experimental data points to the full curve shown in Fig. 4, the values of $\lambda_i = 0.46$ eV and $\kappa = 1$ are obtained. These results indicate an adiabatic electron transfer mechanism. Although the classical model reproduces the experimental results fairly well, the data were also analysed by a semiclassical treatment (see below).

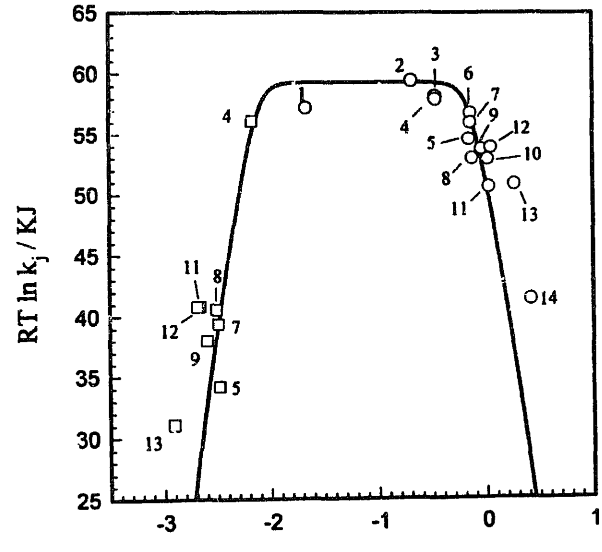

Fig. 4. Plot of $RT\ln k_j$ vs. ΔG for $[Re(CO)_3(4\text{-phenylpyridine})_3^+]^*$–amine system. The open circles represent the forward electron transfer ($j = q$) and the open squares represent the back electron transfer ($j = back$). The full line represents the best-fit correlation of the experimental data in both the normal and inverted regions according to Eq. (17). For $\lambda_{out} = 0.674$ eV, the values obtained from the fitting are $\kappa = 1$ and $\lambda_i = 0.464$ eV.

Plots such as that given in Fig. 4 are difficult to make, since it must be assumed that both the reorganization energies and the electronic coupling of the reactants are the same or very similar (see Scott et al. [32]). In the present example, the reorganization barriers should not be very different due to the fact that the sizes and charges of the reactants for the excited state reaction are similar to those of the ground state reaction. The electronic coupling terms are also similar because the orbitals involved in both reactions are the n orbital from the amine and the π orbital from the 4-phenylpyridine ligand.

3.7. Semiclassical treatment

A semiclassical treatment of electron transfer has been given [33] and discussed in detail [34] elsewhere. The semiclassical expression for the thermally weighted Franck–Condon term is

$$G=(2\pi\lambda h\nu\coth\gamma)^{-1/2}$$
$$\times\exp[-(\Delta G+\lambda)^2/(2\lambda h\nu\coth\gamma)] \qquad (20)$$

The variables in Eq. (20) are the same as those in Eq. (17), and $\lambda h\nu\coth\gamma$ is an abbreviation for $\Sigma_{j=1}^{N}\lambda_j h\nu_j\coth\gamma_j$, where γ_j is $h\nu_j/2kT$. ν_j are the frequencies of the vibrational modes of the acceptor and donor involved in the process. The vibrational modes associated with λ_j for the aromatic amines are commonly chosen between 1000 and 1500 cm^{-1} which are typical of in-plane carbon–carbon skeletal vibration [12]. In the case of tertiary amines, the C–N stretching mode can be considered to be active (1000–1300 cm^{-1}). As in the present case the amines are mostly tertiary, a value of 1100 cm^{-1} has been used. For the rhenium complex, the two vibrational modes used (500 and 1420 cm^{-1}) were those obtained from spectral fitting. However, when the rate constants were fitted (see below) using the three frequencies, the λ_j values associated with the 500 cm^{-1} (complex) and 1100 cm^{-1} (amine) modes became zero. Then the best fitting was obtained by considering only the 1420 cm^{-1} vibrational mode of the complex and a 200 cm^{-1} vibrational mode for the solvent. To calculate the rate constants, we used Eqs. (21) and (22)

$$k_j^{-1}=k_e^{-1}+k_d^{-1} \qquad (21)$$

$$k_e=\kappa Z(4\pi kT\lambda)^{1/2}G \qquad (22)$$

where G is given by Eq. (20) and $\lambda=\Sigma_{j=1}^{N}\lambda_j$ is the sum over the inner- and outer-sphere λ values. Z, the collision frequency in solution, is usually assumed to be approximately 10^{11} M^{-1} s^{-1}. However, a more realistic value can be calculated by Eq. (23) [35]

$$Z=g_0(\sigma)4\pi\sigma^2\nu/\alpha \qquad (23)$$

Using the values of $g_0(\sigma)\approx 1$, $\nu\approx 10^{13}$ s^{-1}, $\alpha\approx 2.6$ Å^{-1} (see Ref. [35]) and $\sigma=(r_A+r_D)=12.9$ Å, a value of $Z=4.8\times10^{12}$ M^{-1} s^{-1} is obtained. This result can be compared with the gas phase hard sphere collision frequency $Z^*=(8\pi kT/\mu)^{1/2}\sigma^2$ for molecules of reduced mass $\mu\approx 110$, which equals 8×10^{11} M^{-1} s^{-1} at 298 K. The κ values obtained (by fitting the experimental k_j values with Eqs. (21) and (22)) with these collision frequencies are 0.27 and greater than unity respectively. This indicates that the hard sphere model is not a good approach. In any case, the electron transfer reaction shows very weak non-adiabaticity.

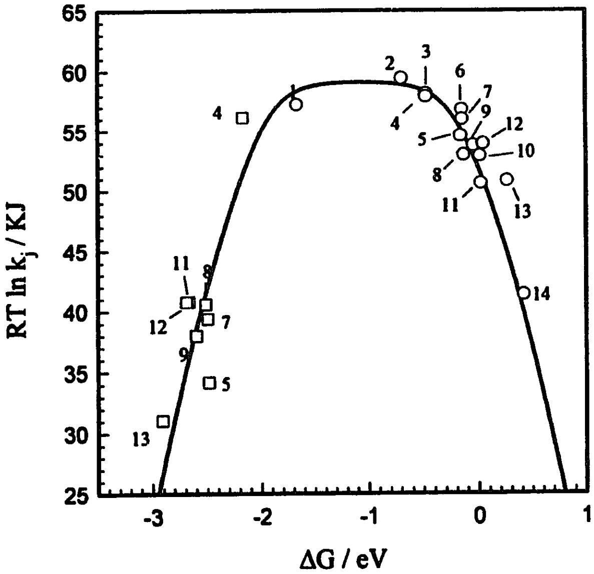

Fig. 5. Plot of $RT\ln k_j$ vs. ΔG for [$Re(CO)_3$(4-phenylpyridine)$_3^+$]*–amine system. The open circles represent the forward electron transfer (j=q) and the open squares represent the back electron transfer (j=back). The full line represents the best-fit correlation of the experimental data in both the normal and inverted regions according to Eqs. (20), (21) and (22). The vibrational frequencies used in the fitting were 1420 cm^{-1} for the rhenium complex and 200 cm^{-1} for the solvent. For $\lambda_{out}=0.674$ eV, the values obtained from the fitting are $\kappa=0.27$ and $\lambda_i=0.40$ eV.

As can be seen in Fig. 5, the semiclassical model reproduces the experimental electron transfer rate constant satisfactorily. However, the k_{back} values (inverted region) present some scattering. This can be attributed to the fact that, to calculate ΔG, the peak oxidation potentials for the amines must be used instead of the reversible redox potential.

The adiabaticity of the electron transfer reaction is influenced by the extent of spatial orbital overlap between the donor and acceptor. Modified extended Hückel calculations [18] performed on $ClRe(CO)_3(4\text{-phpy})_2$ show that, although some high-energy occupied molecular orbitals are linear combinations constructed with even contributions from the Re, Cl, CO and pyridine orbitals, the low-energy unoccupied molecular orbitals are mainly localized in the pyridines. This implies that, when an electron is transferred to the Re complex, it should localize on the pyridine ligand. In this regard, it should be noted that the spectrum of the $Re(CO)_3(4\text{-phpy})_3^{\cdot}$ radical resembles that of the MLCT excited state [16], suggesting structural similarities. As a result, the degree of interaction with the amine cation radical should be important and the reaction should show poor non-adiabaticity.

The value $\lambda_i = S_L h\nu_L + S_M h\nu_M = 0.44$ eV, obtained above by fitting the emission spectra, is very close to that found from a semiclassical fitting of the experimental electron transfer rate constants, $\lambda_i = 0.40$ eV. These results suggest that the amine does not contribute to the inner-sphere reorganization energy. This can be rationalized by considering the electron to be transferred from the non-bonding amine orbital in the forward electron transfer and to that orbital in the backward electron transfer.

The most important feature of the data in Figs. 4 and 5 is the experimental evidence of inverted behaviour. A number of effects can thwart the observation of an inverted region in bimolecular solution reactions [36]:

1. masking by diffusion control;
2. the existence of an alternative mechanism, such as reaction via exciplexes, atom transfer or the formation of an electronically excited product, which reduce the magnitude of ΔG for the elementary step.

Here, masking by diffusion control is not evident; no deviation from Stern–Volmer behaviour is observed in quenching experiments, no atom transfer is expected and no low-lying excited states seem to be available. On the other hand, nuclear tunnelling due to the very high-frequency modes involved is significant, but does not produce a lack of inverted behaviour. In the unique case in which inverted behaviour is clearly observed for a bimolecular reaction [9], the quenching rate constant (forward electron transfer) remains diffusion limited at highly negative ΔG values. However, a paper recently published [37] presents the reaction between cytochrome and the excited states of Ru complexes showing a modest inverted region effect. In our case, the forward electron transfer seems to decrease slightly as the driving force becomes highly exothermic. In an attempt to observe this behaviour more clearly, further studies on single electron transfer reactions involving Re complexes are currently underway in our laboratory.

Acknowledgements

This work was supported in part by the Consejo Nacional de Investigaciones Científicas y Técnicas (CONICET) de la República Argentina, the Comisión de Investigaciones Científicas de la Provincia de Buenos Aires (CICBA) and Fundación Antorchas. E.W. wishes to thank CONICET for a research graduateship. We thank Dr G. Ferraudi from Notre Dame Radiation Laboratory for his cooperation. The emission spectra were taken at INIBIOLP (UNLP). We thank Dr H. Garda for his assistance and for hosting our visits to INIBIOLP.

References

[1] R.A. Marcus, Discuss. Faraday Soc. 29 (1960) 21.
[2] R.A. Marcus, J. Photochem. Photobiol. A: Chem. 82 (1994) 1–3.
[3] J.V. Beitz, R.K. Huddleson, J. Chem. Phys. 71 (1979) 4579. J.R. Miller, J.V. Beitz, R.K. Huddleson, J. Am. Chem. Soc. 106 (1984) 5057. G.L. Closs, L.T. Calcaterra, N.J. Green, K.W. Penfield, J.V. Miller, J. Phys. Chem. 90 (1986) 3673. G.L. Closs, J.R. Miller, Science 240 (1988) 440.
[4] I.R. Gould, D. Ege, S.L. Mattes, S. Farid, J. Am. Chem. Soc. 109 (1987) 3794. I.R. Gould, J.E. Moser, B. Armitage, S. Farid, J. Am. Chem. Soc. 111 (1989) 1917. I.R. Gould, R. Moody, S. Farid, J. Am. Chem. Soc. 110 (1988) 7242.
[5] M.P. Irvine, R.J. Harrison, G.S. Beddard, P. Leighton, J.K.M. Sanders, Chem. Phys. 104 (1986) 315. G. Tapolsky, R. Duesing, T.J. Meyer, J. Phys. Chem. 93 (1989) 3885. P.Y. Chen, R. Duesing, G. Tapolsky, T.J. Meyer, J. Am. Chem. Soc. 111 (1989) 8305. P.Y. Chen, R. Duesing, D.K. Graff, T.J. Meyer, J. Phys. Chem. 95 (1991) 5850.
[6] N. Mataga, T. Asahi, Y. Kanda, T. Okada, T. Kakitani, Chem. Phys. 127 (1988) 249. T. Ohno, A. Yoshimura, N. Mataga, J. Phys. Chem. 90 (1986) 3295. T. Ohno, A. Yoshimura, N. Mataga, J. Phys. Chem. 94 (1990) 4871.
[7] D.Y. Yang, R.I. Cukier, J. Chem. Phys. 91 (1989) 281. M.R. Gunner, P.L. Dutton, J. Am. Chem. Soc. 111 (1989) 3400. T.J. Meade, H.B. Gray, J.R. Winkler, J. Am. Chem. Soc. 111 (1989) 4353. L.S. Fox, M. Kozik, J.R. Winkler, H.B. Gray, Science 247 (1990) 1069.
[8] C. Creutz, N. Sutin, J. Am. Chem. Soc. 99 (1977) 241. T.B. Truong, J. Phys. Chem. 88 (1986) 3906. P.P. Levin, P.F. Pluzhnikov, V.A. Kuzmin, Chem. Phys. Lett. 147 (1988) 283.
[9] T.M. McCleskey, J.R. Winkler, H.B. Gray, J. Am. Chem. Soc. 114 (1992) 6935.
[10] M.S. Wrighton, D.L. Morse, J. Am. Chem. Soc. 100 (1974) 5790. P.J. Giordano, S.M. Fredericks, S.M. Wrighton, D.L. Morse, J. Am. Chem. Soc. 100 (1978) 2257. F. Zingales, U. Satorelli, A. Trovati, Inorg. Chem. 6 (1967) 1246. F. Zingales, M. Graziani, F. Faraone, U. Belluco, Inorg. Chim. Acta 1 (1967) 172. I. Wender, P. Pino (Eds.), Organic Synthesis via Metal Carbonyls, vol. 1, Interscience, New York, 1987. M.S. Wrighton, D.L. Morse, L. Pdungssap, J. Am. Chem. Soc., 97 (1975) 2073.
[11] D. Martire, M.C. Gonzalez, M.R. Féliz, A.L. Capparelli, Int. J. Chem. Kinet. 23 (1991) 457.
[12] D. Burget, P. Jacques, E. Vauthey, P. Suppan, E. Haselbach, J. Chem. Soc., Faraday Trans. 90 (17) (1994) 2481.
[13] C.K. Mann, K.K. Barnes, Electrochemical Reactions in Non-Aqueous Systems, Marcel Dekker, New York, 1970.
[14] R. Ballardini, G. Varoni, M.T. Indelli, F. Scandola, V. Valzani, J. Am. Chem. Soc. 100 (1978) 7219–7223.
[15] H. Sun, M.Z. Hoffman, J. Phys. Chem., 98 (1994) 11 719–11 726.
[16] G. Ruiz, E. Wolcan, M.R. Féliz, J. Photochem. Photobiol. A: Chem. 101 (1996) 119–125.
[17] G. Ruiz, E. Wolcan, A.L. Capparelli, M.R. Féliz, J. Photochem. Photobiol. A: Chem. 89 (1995) 61.
[18] M.R. Féliz, G. Ferraudi, H. Altmiller, J. Phys. Chem. 96 (1992) 258.
[19] F. García-Einschlag, F. Olivetto, A.L. Capparelli, KINESIM, Dirección Nacional del Derecho de Autor, registered No. 701427.
[20] L.I. Grossweiner, M.S. Matheson, J. Phys. Chem. 61 (1957) 1089–1095. R. Devonshire, J.J. Weiss, J. Phys. Chem. 72 (1968) 3815–3820.
[21] J.H. Bexendale, P.L.T. Bevan, D.A. Scott, Trans. Faraday Soc. 64 (9) (1968) 2389–2397.
[22] G. Ferraudi, M.R. Féliz, E. Wolcan, I. Hsu, S.A. Moya, J. Guerrero, J. Phys. Chem. 99 (1995) 4929.
[23] J.V. Caspar, T.D. Westmoleland, G.H. Allen, P.G. Bradley, T.J. Meyer, W.H. Woodruff, J. Am. Chem. Soc. 106 (1984) 3492. G.H. Allen, R.P. White, D.P. Rillema, T.J. Meyer, J. Am. Chem. Soc. 106 (1984) 2613.
[24] J.M. Chen, T.I. Ho, C.V. Mou, J. Phys. Chem. 94 (1990) 2889. C. Creutz, A.D. Keller, N. Sutin, A.P. Zipp, J. Am. Chem. Soc. 104 (1982) 3614.

[25] N. Sutin, Acc. Chem. Res. 15 (1982) 275. N. Sutin, Prog. Inorg. Chem. 30 (1983) 441. D. Sandrini, M. Maestri, P. Belser, A. von Zelewsky, V. Balzani, J. Phys. Chem. 89 (1985) 3675.
[26] R.A. Marcus, J. Phys. Chem. 98 (1994) 5332.
[27] R.A. Marcus, J. Chem. Soc. 24 (1956) 966.
[28] J.A. Riddick and W.B. Bunger, Organic Solvents, Techniques of Chemistry, Wiley Interscience, New York, 3rd Ed., 1979.
[29] J.A. Riddick and W.B. Bunger, Organic Solvents, Techniques of Chemistry, Wiley Interscience, New York, 4th Ed., 1986.
[30] N. Murakami-Iha, G. Ferraudi, J. Chem. Soc., Dalton Trans. (1994) 2565–2571.
[31] M.Z. Smoluchowski, Phys. Chem., 92 (1917) 129.
[32] R.M. Fuoss, J. Am. Chem. Soc. 80 (1958) 5059. M. Eigen, Z. Phys. Chem. 1 (1954) 176. J.R. Scott, A. Willie, M. McLean, P.S. Stayton, S.G. Sliger, B. Durham, F. Millett, J. Am. Chem. Soc. 115 (1993) 6820–6824.
[33] J.J. Hopfield, Proc. Natl. Acad. Sci. USA 71 (1974) 3640. B. Chance, D.C. DeVault, H. Frauenfelder, J.R. Schrieffer, N. Sutin (Eds.), Tunneling in Biological Systems, Academic Press, New York, 1979. E. Roux (Ed.), Electrical Phenomena at the Biological Membrane Level, Elsevier, Amsterdam, 1977.
[34] P. Siders, R.A. Marcus, J. Am. Chem. Soc. 103 (1981) 741. R.A. Marcus, in: T.E. Kin, H.S. Mason, M. Morrison (Eds.), Third International Symposium on Oxidases, 1979.
[35] R.A. Marcus, Int. J. Chem. Kinet. 13 (1981) 865.
[36] R.A. Marcus, Faraday Discuss. Chem. Soc. 74 (1982) 7.
[37] C. Turró, J.M. Zaleski, Y.M. Karabatsos, D.G. Nocera, J. Am. Chem. Soc. 118 (1996) 6060–6067.